JOURNAL OF APPLIED ELECTROCHEMISTRY 25 (1995) 755–763

An efficient method for solving the model equations of a two dimensional packed bed electrode

Y. P. SUN, W. L. XU

Chemical Engineering Department, Taiyuan University of Technology, Shanxi 030024, China

K. SCOTT

Department of Chemical and Process Engineering, University of Newcastle upon Tyne, NE1 7RU, Great Britain

Received 20 May 1992; revised 10 February 1993

A theoretical and experimental study of a flow-by packed bed electrochemical reactor consisting of graphite particles is given. The mathematical model describes the two dimensional distributions of electrode potential and reactant concentration in the reactor, and includes the influence of lateral dispersion between the feeder electrode and membrane. A new efficient numerical method, based on central finite difference and orthogonal collocation is used to solve the model. Results of the model simulations agree well with experimental measurement of the potential distribution for the ferrocyanide/ferricyanide system.

List of symbols

a	specific surface area of packed bed electrode, (cm^{-1})
c_i	concentration of species i ($i = 2$ for cathodic species) ($mol\,dm^{-3}$)
c_{i0}	inlet concentration of species i ($mol\,dm^{-3}$)
C	dimensionless concentration
c_s	concentration on the electrode surface ($mol\,dm^{-3}$)
C_s	dimensionless concentration on the electrode surface
D_e	effective diffusion coefficient ($cm^2\,s^{-1}$)
Da	Damköhler number
F	Faraday's constant (96 487 $C\,mol^{-1}$ of electrons)
i	current density ($A\,m^{-2}$)
i_0	exchange current density ($A\,m^{-2}$)
I	number of equation
j_2	electrochemical reaction rate per unit area ($mol\,cm^{-2}\,s^{-1}$)
J	number of node point
k_a	average local mass transfer coefficient ($cm\,s^{-1}$)
n	number of moles of electrons
N	number of inner collocation points
N_2	flux of species 2 ($mol\,cm^{-2}\,s^{-1}$)
Pe	Peclet number
R	gas constant (8.314 $J\,mol^{-1}\,K^{-1}$)
Sh_m	modified Sherwood number
T	temperature (K)
u_a	average axial velocity ($cm\,s^{-1}$)
x	lateral coordinate (cm)
x_0	electrode depth (cm)
X	dimensionless depth of electrode
y	axial coordinate (cm)
y_0	electrode length (cm)
Y	dimensionless length of electrode
z_0	electrode width (cm)

Greek symbols

α	aspect ratio
α_a	anodic transfer coefficient
α_c	cathodic transfer coefficient
η	overpotential (V)
ν	stoichiometric coefficient
ζ	dimensionless rate constant
σ_2	effective conductivity of electrolyte ($\Omega^{-1}\,cm^{-1}$)
ϕ_1	potential of electrode (V)
ϕ_2	potential of electrolyte (V)
ϕ_{eq}	equilibrium potential (V)
Φ	dimensionless potential

1. Introduction

The area of porous and particulate bed electrodes has been extensively studied with a range of mathematical models developed in attempts to predict the behaviour. Early studies sought analytical solutions of the one dimensional potential distribution model in porous electrodes with activation controlled kinetics [1–3].

Numerous other publications appeared in this area in the late 1960s and 1970s covering electrochemical rate equation governed by either kinetics, mass transport and mixed kinetic and mass transport control and as a result of which several reviews appeared

0021-891X

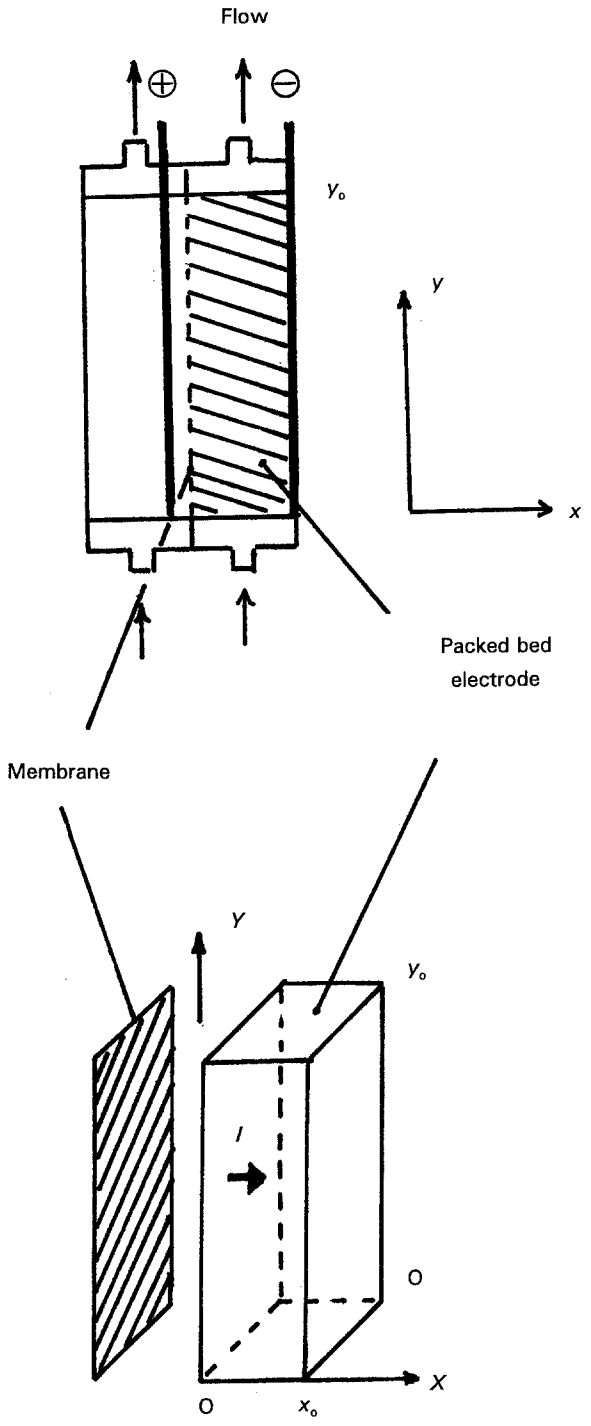

Fig. 1. Schematic diagram of the packed bed electrochemical reactor.

[4–8]. Most of this work considered porous flow through electrode systems for which a one dimensional model is appropriate. The flow by configuration, which is of greater practical significance (in which electrolyte flow and current flow are perpendicular), however, requires a two dimensional model which was analysed less extensively [9–11]. For reaction systems influenced by kinetics and mass transport the numerical solution of the defining equation of porous or particulate electrodes can be particularly demanding.

In electrochemical engineering the mathematical model equations, which describe the concentration and potential distributions in an electrochemical reactor, are usually parabolic and elliptical equations with mixed boundary conditions, respectivley. The set of nonlinear partial differential equations (PDEs) generally cannot be solved by analytical solutions and thus require numerical methods.

The central finite difference method [12] and the orthogonal collocation method [13] are two direct ways of solving the problem, and have been widely applied in chemical engineering modelling. The central finite difference method has a high accuracy in a general case, and can obtain a stable convergence solution. However, its CPU time to reach a proper convergence criterion is rather long for solving the boundary problem involved with a nonlinear elliptical equation in an electrochemical engineering model. On the contrary, the orthogonal collocation method has advantages of a shorter CPU time and less prior treatment before run time on a computer, but cannot achieve a stable convergence solution with ease. For these reasons, a numerical method having the advantages of these two methods is developed in the present work. It provides an efficient way to solve a mathematical model of a two dimensional packed bed electrode reactor. The model is used to predict two dimensional electrode potential and concentration distributions and experimental measurements of potential distribution generally agree with prediction.

2. Mathematical model of a packed bed electrode reactor

A general packed bed electrode reactor with a rectangle geometry is discussed. The schematic diagram is shown in Fig. 1. The assumptions used in the development of the model are:

(i) Dilute solution theory is applied since a packed bed electrode reactor is suitable for the treatment of a low concentration of reacting ions. Sufficient supporting electrolyte is present, so that ionic migration of reacting species is neglected.
(ii) The electrolyte and electrode are both treated as continuous phases.
(iii) Isothermal conditions exist.
(iv) The porosity and specific area of the electrode are uniform, and do not change with time.
(v) Dispersion is absent in the axial direction.
(vi) The concentration of the anodic reactant is large relative to the concentration of the cathodic reactant.
(vii) The electrochemical kinetic expression follows a Butler–Volmer type relationship.

A Poisson equation can be used to describe the potential distribution within the electrolyte phase in the packed bed. The potential $\phi_{1(x,y)}$ at any point of the electrode is uniform because the effective conductivity of the electrode phase is high.

The distribution of the potential of the electrolyte phase $\phi_{2(x,y)}$ can be expressed by Ohm's law as

$$\nabla^2\phi_2 = -\nabla i_2/\sigma_2 \tag{1}$$

where σ_2 is the effective conductivity of the electrolyte. i_2 is the current density in the electrolyte. According to the model assumptions, the expression of $i_{2(x,y)}$ is

$$j_{2(x,y)} = i_0\left\{\frac{c_{1(x,y)}}{c_{10}}\exp\left[\alpha_a\left(\frac{nF}{RT}\right)\eta\right] - \frac{c_{2(x,y)}}{c_{20}}\exp\left[-\alpha_c\left(\frac{nF}{RT}\right)\eta\right]\right\} \tag{2}$$

where i_0 is the exchange current density, α_a and α_c are transfer coefficients and the subscripts '0' on the concentrations C_1 and C_2 refer to inlet conditions.

With the assumption (vi), the change in concentration of the anodic reactant is negligible ie $c_{1(x,y)} = c_{10}$ then Equation 2 can be simplified:

$$j_{2(x,y)} = i_0\left\{\exp\left[\alpha_a\left(\frac{nF}{RT}\right)\eta\right] - \frac{c_{2(x,y)}}{c_{20}}\exp\left[-\alpha_c\left(\frac{nF}{RT}\right)\eta\right]\right\} \tag{3}$$

The expression for overpotential η is written as

$$\eta = \phi_1 - \phi_{2(x,y)} - \phi_{eq} \tag{4}$$

where ϕ_{eq} refers to the equilibrium potential, namely the open circuit potential calculated with these values of inlet concentrations.

The equation for the conservation of charge is

$$\nabla \cdot j_2 = -aj_2 \tag{5}$$

where aj_2 is the local current per unit volume of the electrode.

Substitution of Equation 5 into Equation 1 yields the following equation describing the potential distribution of the electrolyte phase:

$$\nabla^2\phi_2 = -aj_2/\sigma_2 \tag{6}$$

and Equation 6 can be rewritten as

$$\nabla^2\eta = aj_2/\sigma_2 \tag{7}$$

A steady state material balance for the cathodic species 2 in an element of the packed bed electrode of volume, $dx\,dy\,z_0$, is

$$-\nabla N_2 + aj_2 = 0 \tag{8}$$

For a two dimensional system with a linear velocity in the y-direction only and in the absence of axial dispersion Equation 8 can be simplified to

$$D_e\frac{\partial c^2_{2(x,y)}}{\partial x^2} - u_a\frac{\partial c_{2(x,y)}}{\partial y} = \frac{vaj_{2(x,y)}}{nF} \tag{9}$$

where c_2 is the local reactant concentration, and u_a is the superficial electrolyte velocity. The lateral dispersion is characterised by an effective diffusion coefficient D_e.

Under steady state conditions, the local reaction rate is equal to the local mass transfer rate, expressed as

$$\frac{vaj_{2(x,y)}}{nF} = k_a a(c_2 - c_{2s}) \tag{10}$$

where k_a is the mass transfer coefficient. Different expressions of k_a should be used for different ranges of Reynolds number Re [14].

An appropriate set of boundary conditions is as follows:

reactor inlet

$$y = 0, \quad 0 \leqslant x \leqslant x_0, \quad c_2 = c_{20}, \quad \partial\phi_2/\partial y = 0 \tag{11}$$

reactor exit

$$y = y_0, \quad 0 \leqslant x \leqslant x_0, \quad \partial c_2/\partial y = 0, \quad \partial\phi_2/\partial y = 0 \tag{12}$$

membrane

$$x = 0, \quad 0 \leqslant y \leqslant y_0, \quad \partial c_2/\partial x = 0, \quad \phi_2 = \text{constant} \tag{13}$$

feeder

$$x = x_0, \quad 0 \leqslant y \leqslant y_0, \quad \partial c_2/\partial x = 0, \quad \partial\phi_2/\partial y = 0 \tag{14}$$

Equations 7, 9 and 10 can be simplified by defining the following dimensionless variables:

$$X = x/x_0, \; Y = y/y_0, \; C = c_2/c_{i0}, \; \Phi = nF\eta/RT \tag{15}$$

Dimensionless equations for Equations 7, 9 and 10 are as follows:

$$\frac{\partial^2\Phi}{\partial X^2} + \alpha^2\frac{\partial^2\Phi}{\partial Y^2} = \xi[\exp(\alpha_a\Phi) - C_s\exp(-\alpha_c\Phi)] \tag{16}$$

$$\frac{\partial^2 C}{\partial X^2} - Pe\alpha\frac{\partial C}{\partial Y} = Sh_m(C - C_s) \tag{17}$$

$$Da[\exp(\alpha_a\Phi) - C_s\exp(-\alpha_c\Phi)\} = (C - C_s) \tag{18}$$

with corresponding boundary conditions:

$$Y = 0, \quad 0 \leqslant X \leqslant 1, \quad C = 1, \quad \frac{\partial\Phi}{\delta Y} \tag{19}$$

$$Y = 1, \quad 0 \leqslant X \leqslant 1, \quad \frac{\partial C}{\delta Y} = 0, \quad \frac{\partial\Phi}{\delta Y} = 0 \tag{20}$$

$$X = 0, \quad 0 \leqslant Y \leqslant 1, \quad \frac{\partial C}{\delta X} = 0, \quad \Phi = \text{constant} \tag{21}$$

$$x = 1, \quad 0 \leqslant y \leqslant 1, \quad \frac{\delta C}{\delta X} = 0, \quad \frac{\delta\Phi}{\delta X} = 0 \tag{22}$$

The boundary condition at the membrane, $X = 0$, is selected to conform with the experimental imposed condition of operation. This condition is consistent with the work of Alkire and Ng [9] on two dimensional potential distributions in packed bed electrodes. Experimental measured potential confirm that this is an accurate representation of the boundary.

The Butler–Volmer kinetic Equation 16 was selected on the basis of conforming with the model assumptions. There are five dimensionless groups in the model equations:

aspect ratio

$$\alpha = \frac{x_0}{y_0} \tag{23}$$

dimensionless rate constant

$$\zeta = \frac{i_0 nFax_0^2}{\sigma_2 RT} \tag{24}$$

Peclet number

$$Pe = \frac{u_a x_0}{D_e} \tag{25}$$

modified Sherwood number

$$Sh_m = \frac{k_a a x_0^2}{D_e} \tag{26}$$

Damköhler number

$$Da = \frac{i_0 \nu}{nFk_a c_0} \tag{27}$$

Equation 16 describing the potential distribution in the packed bed, is an elliptical one, while Equation 17, describing the concentration distribution, is a parabolic one. Both of these satisfy the mixed boundary conditions and involve the nonlinear terms, $\exp(\alpha_a\Phi)$, $\exp(\alpha_c\Phi)$ associated with the electrode potential.

The significance of the dimensionless parameters has been discussed in previous publications [9, 10]. ζ contains the ratio i_0/σ_2 and indicates the relative importance of electrolyte resistance and charge-transfer resistance. In the absence of mass transport limitations ζ is the parameter that controls electrode behaviour and can be regarded as a linear polarization parameter. When $\zeta < 1$, the conductivity is sufficiently high so that the secondary current distribution is uniform. *Pe* determines the relative importance of convective transport to diffusive transport of reactants. If *Pe* is large, the current distribution along the axial direction will be uniform since the supply of reactions will insure against depletion. For lower values of *Pe*, axial distributions will be non-uniform due to depletion of reactant.

In the operation of packed bed electrodes there are two limiting situations which may arise in practice associated with either a complete mass transport control of the reaction or complete kinetic control of the reaction. In both cases analytical solutions can be obtained which enables the accuracy of the numerical solution to be determined.

In the system an important dimensionless group is the Damköhler number *Da* which is a measure of the ratio of the kinetic rate to the mass transfer rate. An increase in the values of *Da* (*and* Φ), causes the concentration difference $(c - c_s)$ between the local electrolyte and electrode surface to become large, namely c_s will be close to zero. In this case, the reaction process in the packed bed will be increasingly controlled by mass transfer and then the model can be simplified as

$$Pe \propto \frac{dC}{dY} = -Sh_m C \tag{28}$$

$$\frac{\partial^2\Phi}{\partial X^2} + \alpha^2 \frac{\partial^2\Phi}{\partial Y^2} = \frac{\zeta}{Da} C \tag{29}$$

where no nonlinear terms exist, so an analytical solution can be obtained by using Fourier transformation [16]. At the other extreme on decreasing the values of *Da* and Φ, the concentration difference $(c - c_s)$ will be close to zero (ie $c = c_s$). In this case, the reaction process in the packed bed is controlled by the electrode kinetic reaction rate, and the model can be simplified to the dimensionless form

$$\frac{d^2\Phi}{dX^2} = \zeta[\exp(\alpha_a\Phi) - C\exp(-\alpha_c\Phi)] \tag{30}$$

This latter case is applicable to a reactor with a low conversion per pass, and has been previously analysed by several authors [17, 18].

3. Numerical method for solving the model equations

The set of PDEs, Equations 16 and 17, is first converted into a set of ODEs by orthogonal collocation [13]. According to the principle of the orthogonal collocation method, values of first order and second order derivatives can be evaluated in terms of linear combination of values of trial functions by using collocation matrices, A_c and B_c, at collocation points. The ordinary differential equations obtained from Equations 16 and 17, are therefore accordingly written:

$$\frac{d^2\Phi(I)}{dX^2} + \alpha^2 \sum_{K=1}^{N+2} B_c(I,K) \times \Phi(K) = \frac{\zeta}{Da}[C(I) - C_s(I)] \tag{31}$$

$$\frac{d^2C(I)}{dX^2} - Pe\alpha \sum_{K=1}^{N+2} A_c(I,K) \times \Phi(K) = Sh_m[C(I) - C_s(I)] \tag{32}$$

where I refers to the number of the equation, of which there are $N + 2$ including two boundary conditions, N is the number of inner collocation points; K is the number of collocation points, $K = 1, 2, \ldots N + 2$.

Villadsen [13] presents the computer programs which can be used to evaluate zeros (as collocation points) of orthogonal polynomial and collocation matrices A_c, B_c. If values of A_c and B_c are known, X will be considered the only independent variable in the ODEs.

Further discretization of derivatives in Equations 31 and 32 can be done by using the central finite difference method. This is now described below treating

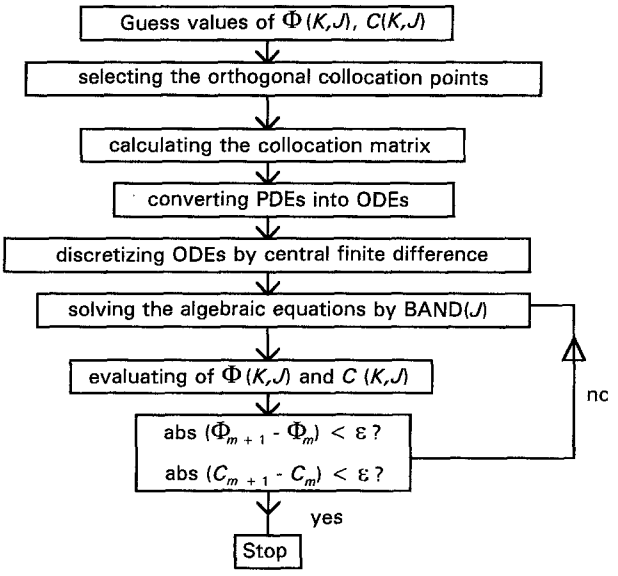

Fig. 2. Flowchart for the numerical solution of the two dimensional model.

Equation 31 as an example:

$$\frac{d^2\Phi(I)}{dX^2} = [\Phi(I,j+1) + \Phi(I,j-1) - 2\Phi(I,j)]/(\Delta X)^2 \tag{33}$$

where j refers to the mesh point number.

Newman [12] outlines the procedure for expressing any ordinary differential equation into finite difference form. Substitution of Equation 33 into Equation 31, therefore, yields the following algebraic equation:

$$\sum_{K=1}^{N+2} A(I,K)\Phi(K,J-1) + \sum_{K=1}^{N+2} B(I,K)\Phi(K,J) + \sum_{K=1}^{N+2} D(I,K)\Phi(K,J+1) - G(I) = 0 \tag{34}$$

For a nonlinear equation, coefficient A, B, C, D and G will be functions not only of the independent variable of X, but also of the dependent variables of $\Phi(K)$. It is necessary to put the nonlinear equation in linear form and iterate over the nonlinearities. The function defined by Equation 34 is called $F(I)$. If one estimates a set of $\Phi(K,J)$ as a trial solution, $F(I)$ can be represented by a Taylor series keeping only the first order terms:

$$F(I) = F(I)^0 + \sum_{K=1}^{N+2} \sum_{M=J-1,J,J+1} \left(\frac{\partial F(I)}{\partial \Phi(K,M)}\right)^0 \times [\Phi(K,M) - \Phi(K,M)^0] \tag{35}$$

The coefficients values in Equations 34 will be as follows:

$$A(I,K) = \left(\frac{\partial F(I)}{\partial \Phi(K,J-1)}\right)^0 \tag{36}$$

$$B(I,K) = \left(\frac{\partial F(I)}{\partial \Phi(K,J)}\right)^0 \tag{37}$$

Table 1. System properties

n	1
$\sigma(\Omega\ \mathrm{cm})^{-1}$	0.108
μ (g cm^{-1} s^{-1})	9.9×10^{-3}
ρ (g cm^{-3})	1.0445
d_p (m)	4×10^{-3}
i_0 (A cm^{-2})	10^{-2}

$$D(I,K) = \left(\frac{\partial F(I)}{\partial \Phi(K,J+1)}\right)^0 \tag{38}$$

$$G(I) = -F(I)^0 + \sum_{K,M}^{N+2} \left(\frac{\partial F(I)}{\partial \Phi(K,M)}\right)^0 \Phi(K,M)^0 \tag{39}$$

Newman's subroutine BAND(J) [12] works by giving the numerical values of A, B, C, D, and G for each value of J, and by inverting any set of tridiagonal matrixes. Although the technique for using BAND(J) appears simple once the Newman's concept is fully grasped, use of Bennion's subroutine DIFEQ [19] is suggested; this can handle all the linearization and details associated with calling BAND(J).

The mass balance Equation 17 and the boundary condition equations can be treated in similar ways. The total number of equations is $(N+2)*2$. Since there are two dependent variables Φ and C. The numerical procedure is as shown in Fig. 2.

In this program, the guessed values of $\Phi(K,J)$ and $C(K,J)$ are given first and then the collocation points and the collocation matrixes A_c, B_c are calculated by Villadsen's subroutines [13]. Hence, the PDEs are converted into ODEs with respect only to X. The nonlinear ODEs are discretized and linearized by Bennion's DIFEQ [11]. Finally, a set of algebraic equations are solved by Newman's BAND(J) [12].

For solving the model equation, typically four inner collocation points were used in the Y direction, and 21 node points used in the X direction. The convergence criteria was 1.0×10^{-5}. Typical execution times were 20 s per case on an AST 386 computer.

In this program, the trial values of $\Phi(K,J)$ and $C(K,J)$ are selected first and then the collocation points and the collocation matrix are calculated by the orthogonal collocation method. Therefore, the PDEs are converted into ODEs with respect to position X. The nonlinear ODEs are discretized and linearized by the central finite difference method. Finally, a set of algebraic equations are solved by Newman's BAND(J) [1].

For solving the model equation, four inner collocation points were used in the Y direction, and 21 node points used in the X direction. The convergence criteria was 1.0×10^{-5} with eight iterations on an AST 386 computer.

4. Results and discussion

A mathematical model of a packed bed electrode reactor for the system $[Fe(CN)_6]^{-3}/[Fe(CN)_6]^{-4}$ was

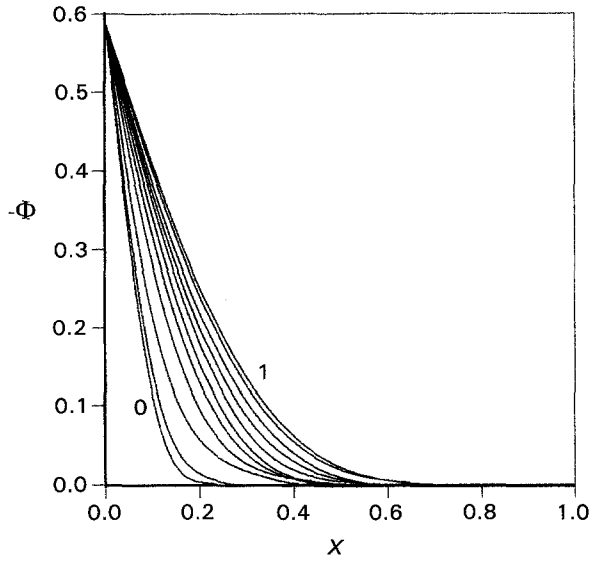

Fig. 3. Distribution of dimensionless electrode potential, Φ in the lateral and axial direction. $\zeta = 0.14 \times 10^5$, $Pe = 0.625 \times 10^6$, $Sh_m = 0.218 \times 10^7$, $Da = 199$, $-\Phi = 0.6$. Curves show axial position varying from $Y = 0$ to 1.0 in increments of 0.1.

calculated by the numerical method presented in this paper. The packed bed electrode has a size of $x_0 = 0.03\,\text{m}$, $y_0 = 0.15\,\text{m}$, $z_0 = 0.06\,\text{m}$, and the electrode material was graphite particles, 4.0 mm in diameter. Sodium hydroxide solution was used as a supporting electrolyte. The concentration of $K_4Fe(CN)_6$ was 100 times higher than that of the $K_3Fe(CN)_6$. The potentials of the electrolyte were measured by eight probes equally positioned along the electrode, to obtain the potential values in the Y direction simultaneously [15]. The probes could be moved in the X direction and were connected to a data acquisition system. The values of input parameters for this system are summarized in Table 1.

The selected operating potential of the packed bed will largely determine the distribution of electrode potential and concentration in its structure. At low applied potentials the reaction will primarily be

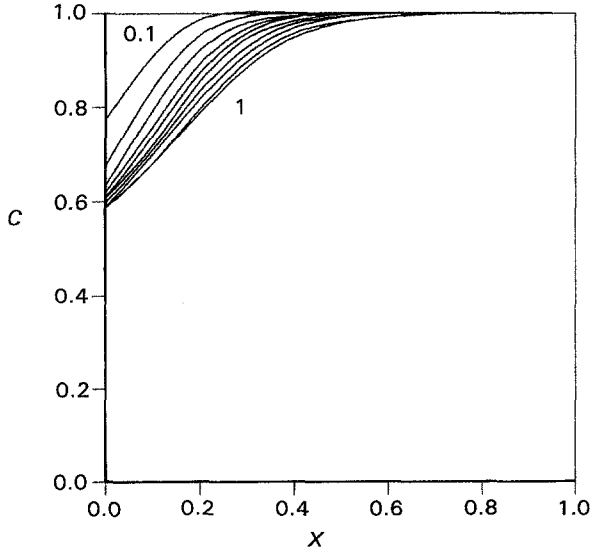

Fig. 4. Distribution of dimensionless concentration C on the packed bed electrochemical reactor. Conditions as in Fig. 3.

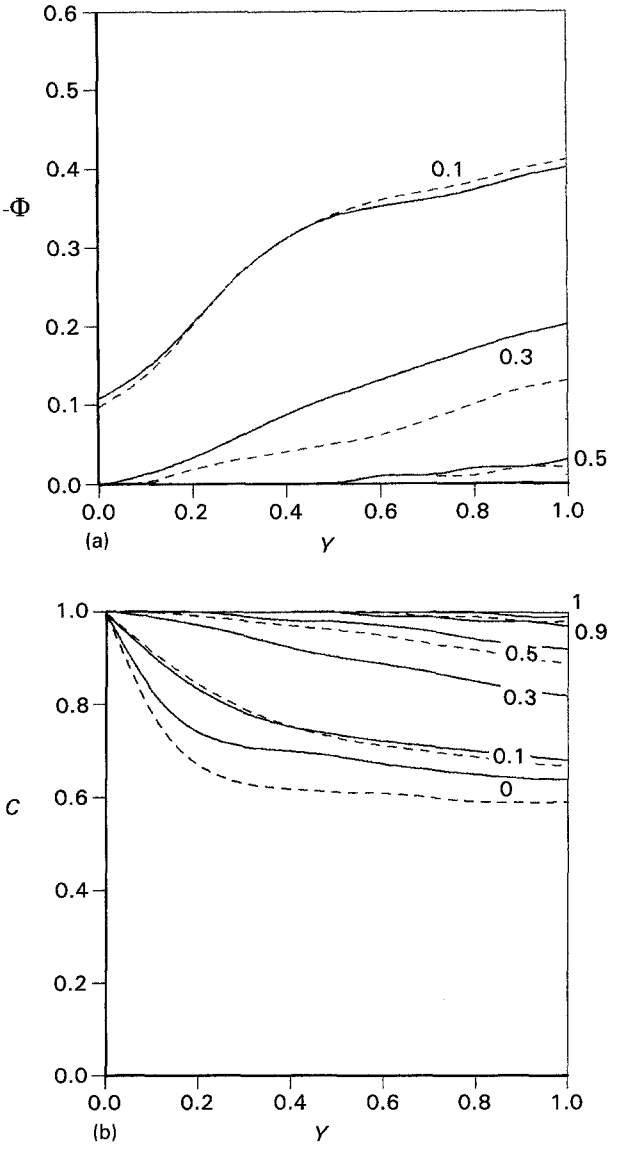

Fig. 5. The effect of dispersion on the distribution of dimensionless concentration and dimensionless potential on the packed bed electrochemical reactor. Values of X on figure. (——): $Pe = 100$, $Sh_m = 349$, $\zeta = 140$; (- - -): $Pe = 6.25 \times 10^5$, $Sh_m = 2.18 \times 10^6$, $\zeta = 0.14 \times 10^5$.

under kinetic control and thus mass transport will only have a small effect on the system as there will not be a large distribution in concentration, due to relatively low conversions achieved.

Figure 3, shows typical potential distributions obtained from the model of the packed bed electrode at a low applied potential. The distributions show that the electrochemical activity is confined to regions closer to the membrane, as expected. The distribution of potential obtained at the axial position $Y = 0$ is in agreement with that predicted by the analytical solution of the model [18] defined in terms of Equation 30, the one dimensional approximation. The distribution of potential is more uniform as the downstream position of the reactor is approached $Y \rightarrow 1$. An effect of these distributions in potential is that the depletion of reactant is greater as $X \rightarrow 0$ and $Y \rightarrow 1$, which is illustrated in the concentration distributions shown in Fig. 4.

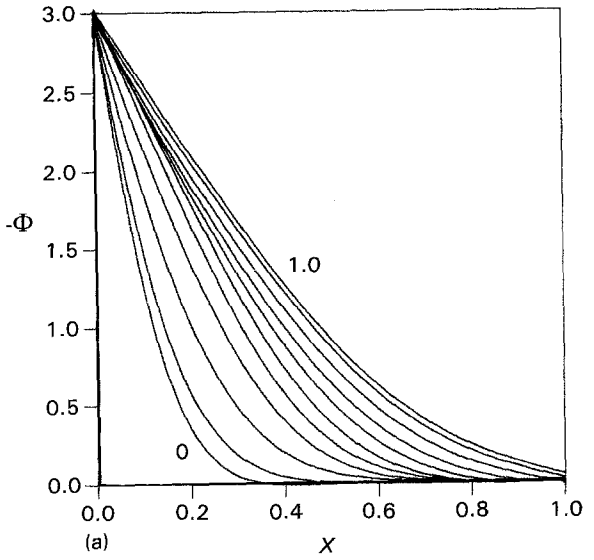

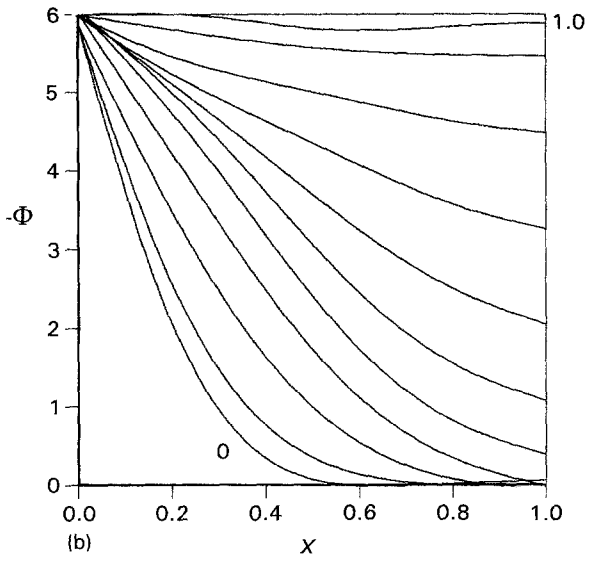

Fig. 6. The distribution of dimensionless potential Φ on the lateral direction at medium and high applied potentials. (a) $\Phi = 3.0$ V (b) $\Phi = 6.0$ V. Other conditions are as in Fig. 3. Values of Y vary from 0 to 1.0 in increments of 0.1.

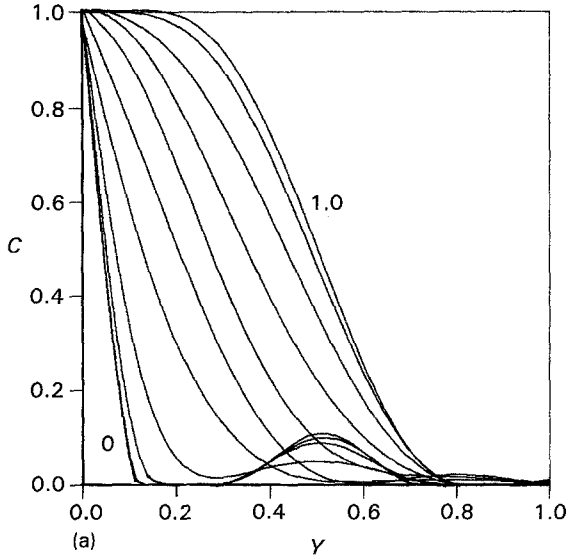

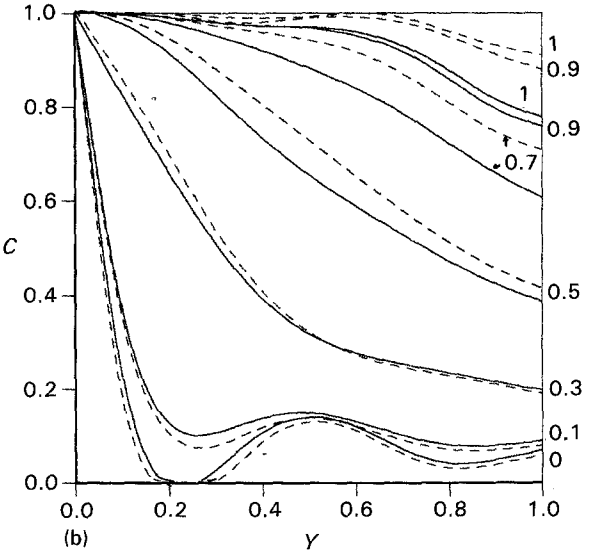

Fig. 7. Distribution of dimensionless concentration C in the packed bed electrochemical reactor at high applied potential. (a) $\Phi = 6.0$ V, $Pe = 1.25 \times 10^5$, $Sh_m = 8.86 \times 10^5$, $Da = 49.1$. Values of position X marked on figure (in increments of 0.1). (b) $\Phi = 3.0$ V, (- - -): parameter values as in (a); (——): $Pe = 100$, $Sh_m = 524$, $Da = 33.3$.

The distributions of Figs 3 and 4 are obtained for a low value of effective diffusivity, of a value equivalent to the ionic diffusivity. The actual value of effective diffusivity is difficult to estimate in packed beds and previous work [9, 10] with packed bed electrochemical reactors has tended to ignore the influence of dispersion on effective diffusivity. Estimations of dispersions coefficients from correlations obtained for packed bed reactors put the value of Peclet number at approximately 100. Figure 5 shows the influence of an increase in effective diffusion coefficient (lower Pe) on the distributions of concentration and electrode potential. The effect of dispersion is to increase the movement of reactant in the lateral direction to offset any depletion in reactant, resulting in a higher concentration of reactant compared to that with low dispersion, especially in this system at regions near the membrane.

The effect of increasing the applied potential on the potential distribution can be seen by comparing Fig. 3 and Fig. 6. The higher the applied potential the more uniform the electrode potential becomes, with a greater proportion of the electrode becoming more active. At an applied potential of 6 V, it is seen that at the downstream position of the reactor ($Y \rightarrow 1$) the electrode potential is quite uniform over the bed thickness. A factor which contributes to this uniformity in potential distribution is the depletion of reactant in the downstream positions of the reactor; as evidenced by the typical concentration distribution depicted in Fig. 7.

A notable feature of the concentration distribution is that at regions close to the membrane a maximum in the concentration occurs approximately half way along the axial position Y. This occurs when the concentration falls to close to zero and then lateral dispersion increases, causing a replenishment in concentration further downstream. As the concentration increases the depletion by reaction, which is in a

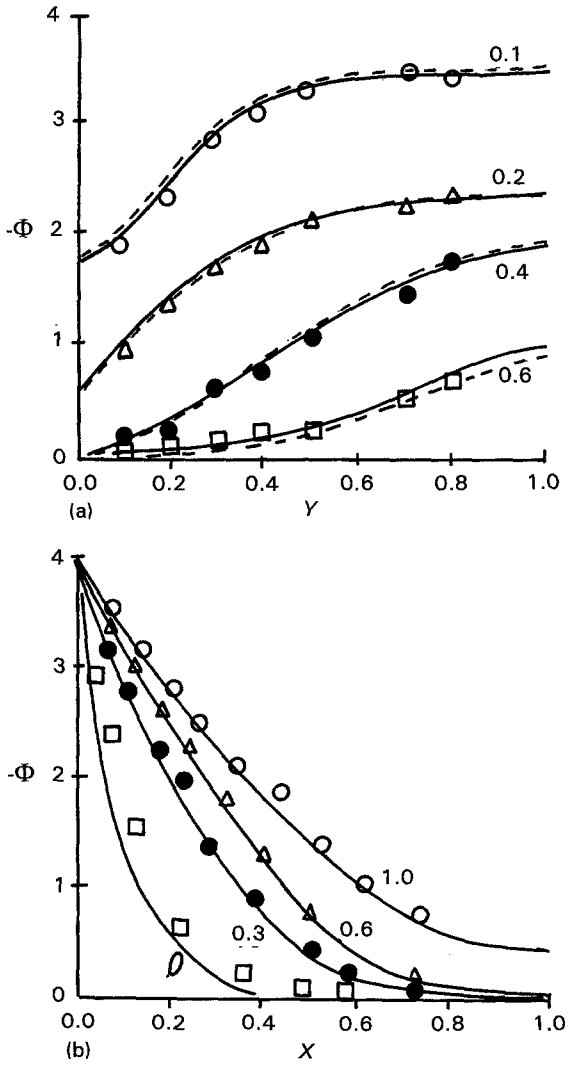

Fig. 8. Experimental potential distribution in the packed bed electrochemical reactor. $U_a = 5 \times 10^{-3}$ ms^{-1}, $\Phi = 4.0$ V, $\zeta = 1.4 \times 10^4$. Model (——): $Pe = 300$; (- - -): $Pe = 1.25 \times 10^5$. (a) Axial potential distribution, (b) lateral potential distributions. (O) Experimental data.

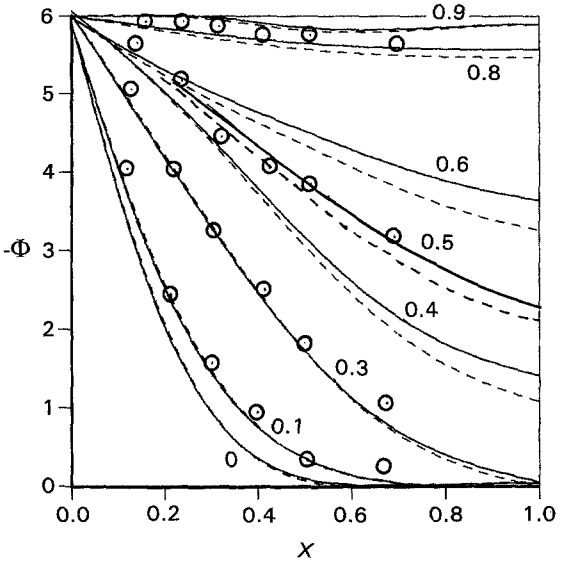

Fig. 9. Experimental potential distributions in the packed bed reactor. $U_a = 10^{-3}$ ms^{-1}, $\Phi = 6.0$ V, $\zeta = 1.4 \times 10^4$. Model (——): $Pe = 100$; (- - -): $Pe = 1.25 \times 10^5$.

mass transport limiting range, increases causing the concentration to fall again further downstream in the Y direction.

Also shown in Fig. 7(b) are the concentration distribution at a lower applied potential (3 V) in which the reaction rate is a mixed kinetic and mass transfer effect. In this case the lateral dispersion is more significant than the reaction rate (cf. $\phi = 6.0$ V) and thus the occurrence of the maxima is more pronounced near the membrane. A change in the dispersion rate has only a relatively small effect on the concentration distribution, as it affects the values of both the Peclet number and Sherwood number.

4.1. *Experimental potential distributions*

Figure 8 shows experimentally measured potential distributions for the packed bed at an applied potential of 4.0 V. The data conform to the theoretical behaviour with the bed being more electroactive at the membrane and the distribution of potential being more uniform near the exit of the reactor. The theoretical distributions in potential are not particularly sensitive to the value of the Peclet number at this value of applied potential as shown in Fig. 8.

Figure 9 shows experimental potential distributions for the packed bed at a higher applied potential of 6.0 V. The data are in general agreement with simulation although it is less satisfactory at higher values of lateral position X and axial position Y. Figure 9 also shows that there is a small influence of dispersion on the potential distribution, with lower Peclet numbers (higher effective diffusion coefficient) tending to make the potential distribution more uniform.

The experimental data and model distributions show a better agreement at low Peclet number where dispersion is more significant, and which is likely to more faithfully represent experimental behaviour.

5. Conclusion

This work has demonstrated the usefulness of an improved numerical method for the solution of a mathematical model for a two dimensional packed bed reactor. The experimental model reaction system is shown to generally substantiate the validity of the mathematical model. This is a general model in that it is applicable to mixed kinetic and mass transport control and is not limited by assumptions of complete mass transport or kinetic rate control. This is an important factor for packed bed type reactors which are being increasingly used in wastewater and effluent treatment applications. The operation below a mass transport controlled condition is ideally required to achieve overall good efficiencies at high conversion, to minimise energy consumption and to reduce operational difficulties associated with secondary processes.

References

[1] J. S. Newman and C. E. Tobias, *J. Electrochem. Soc.* **109** (1962) 1183.
[2] F. A. Posey, *ibid.* **111** (1964) 1173.
[3] M. Poulin, D Hutin and F. Couret, *ibid.* **124** (1977) 180.
[4] R. de Levie, 'Advances in Electrochemistry and Electrochemical Engineering', Vol. 6 (edited by P. Delahay (1967) p. 329.
[5] J. S. Newman and W. Tiedemann, *AIChEJ.* **21** (1975) 25.
[6] J. S. Newman and W. Tiedemann, *Adv. Electrochem. & Electrochem. Engng.* **11** (1978) 353.
[7] F. Couret and A. Storck, 'Elements de Genie Electrochimique' Rec. and Doc., Lavoisier, France (1989).
[8] F. Goodridge and A. R. Wright, Porous Flow-through and Fluidised Bed Electrodes *in* 'Comprehensive Treatise of Electrochemistry' Vol 6, (edited by E. Yeager, J. O. M. Bockris and S. Sarangapani), Plenum Press, London (1983).
[9] R. Alkire and P. K. Ng, *J. Electrochem. Soc.* **124** (1977) 1220.
[10] *Idem, ibid.* **121** (1974) 95.
[11] M. Fleischmann and R. E. W. Jansson, *Electrochim. Acta* **27** (1982) 1029.
[12] J. Newman, 'Electrochemical Systems' Prentice-Hall, Englewood Cliffs, NJ (1973).
[13] J. Villadsen, 'Solution of Differential Equation Models by Polynomial Approximation', Prentice-Hall, Englewood Cliffs, NJ (1978).
[14] D. J. Pickett, 'Electrochemical Reactor Design', Elsevier Scientific, Amsterdam, (1979).
[15] N. L. Weinberg, 'Technique of Electroorganic Chemistry', Vol. 3, Part one, John Wiley & Sons, New York (1983).
[16] A. Storck, M. A. Enriquez-Granados and M. Roger, *Electrochimica Acta* **27** (1982) 293.
[17] K. Scott, *J. Appl. Electrochem.* **16** (1986) 768.
[18] F. A. Posey, *J. Electrochem. Soc.* **111** (1964) 1173.
[19] D. Bennion, *A.I.Chem.E. Symposium Series No. 229*, **79** (1983).